







# Alcohol-Induced Liver Injury: Down-regulation and Redistribution of Rab3D Results in Atypical Protein Trafficking

Carol A. Casey <sup>1,2</sup>, Amanda J. Macke <sup>3</sup>, Ryan R. Gough,<sup>1-3</sup> Artem N. Pachikov <sup>3,4</sup>, Mary E. Morris <sup>3</sup>, Paul G. Thomes <sup>1,2</sup>, Jacy L. Kubik,<sup>1,2</sup> Melissa S. Holzapfel,<sup>5</sup> and Armen Petrosyan <sup>3,4</sup>

Previous work from our laboratories has identified multiple defects in endocytosis, protein trafficking, and secretion, along with altered Golgi function after alcohol administration. Manifestation of alcohol-associated liver disease (ALD) is associated with an aberrant function of several hepatic proteins, including asialoglycoprotein receptor (ASGP-R), their atypical distribution at the plasma membrane (PM), and secretion of their abnormally glycosylated forms into the bloodstream, but trafficking mechanism is unknown. Here we report that a small GTPase, Rab3D, known to be involved in exocytosis, secretion, and vesicle trafficking, shows ethanol (EtOH)-impaired function, which plays an important role in Golgi disorganization. We used multiple approaches and cellular/animal models of ALD, along with Rab3D knockout (KO) mice and human tissue from patients with ALD. We found that Rab3D resides primarily in *trans*- and *cis*-faces of Golgi; however, EtOH treatment results in Rab3D redistribution from *trans*-Golgi to *cis*-medial-Golgi. Cells lacking Rab3D demonstrate enlargement of Golgi, especially its distal compartments. We identified that Rab3D is required for coat protein I (COPI) vesiculation in Golgi, and conversely, COPI is critical for intra-Golgi distribution of Rab3D. Rab3D/COPI association was altered not only in the liver of patients with ALD but also in the donors consuming alcohol without steatosis. In Rab3D KO mice, hepatocytes experience endoplasmic reticulum (ER) stress, and EtOH administration activates apoptosis. Notably, in these cells, ASGP-R, despite incomplete glycosylation, can still reach cell surface through ER-PM junctions. This mimics the effects seen with EtOH-induced liver injury. **Conclusion:** We revealed that down-regulation of Rab3D contributes significantly to EtOH-induced Golgi disorganization, and abnormally glycosylated ASGP-R is excreted through ER-PM connections, bypassing canonical (ER→Golgi→PM) anterograde transportation. This suggests that ER-PM sites may be a therapeutic target for ALD. (*Hepatology Communications* 2022;6:374-388).

The clinical-histologic spectrum of alcohol-associated liver disease (ALD) includes fatty liver, alcoholic steatohepatitis, and cirrhosis. Additionally, steatosis is associated with impaired trafficking of hepatic proteins and their abnormal posttranslational modification.<sup>(1)</sup> Although ethanol

(EtOH)-induced Golgi disorganization in hepatocytes is a well-known phenomenon, in recent years, studies from Petrosyan's laboratory have shown that this process is initiated by dysfunction of SAR1A GTPase followed by altered coat protein II (COPII) vesicle formation and impaired dimerization of the

*Abbreviations:* 3D, three-dimensional; ALD, alcohol-associated liver disease; ASGP-R, asialoglycoprotein receptor; ASH, alcoholic steatohepatitis; ATF6, activating transcription factor 6; COP, coat protein; Ctrl, control; DAPI, 4',6-diamidino-2-phenylindole; EM, electron microscopy; Endo H, endoglycosidase H; ER, endoplasmic reticulum; EtOH, ethanol; IF, immunofluorescence; IRE1, inositol-requiring enzyme 1; KD, knockdown; KO, knockout; NMIIB, nonmuscle myosin IIB; PERK, protein kinase RNA-like endoplasmic reticulum kinase; PLA, proximity ligation assay; PM, plasma membrane; PM-ASGP-R, plasma membrane-associated ASGP-R; SIM, structured illumination superresolution microscopy; siRNA, small interfering RNA; UPR, unfolded protein response; WT, wild type.

Received May 18, 2021; accepted August 5, 2021.

Additional Supporting Information may be found at [onlinelibrary.wiley.com/doi/10.1002/hep4.1811/supinfo](https://onlinelibrary.wiley.com/doi/10.1002/hep4.1811/supinfo).

Supported by a VA Merit Award (I01BX004171) and the National Institute on Alcohol Abuse and Alcoholism (R01AA020735 and R01AA027242).

© 2021 The Authors. *Hepatology Communications* published by Wiley Periodicals LLC on behalf of American Association for the Study of Liver Diseases. This is an open access article under the terms of the Creative Commons Attribution-NonCommercial-NoDerivs License, which permits use and distribution in any medium, provided the original work is properly cited, the use is non-commercial and no modifications or adaptations are made.

View this article online at [wileyonlinelibrary.com](https://onlinelibrary.wiley.com).

key Golgi matrix protein giantin.<sup>(2)</sup> The latter circumstance blocks the fusion of the Golgi membranes, thus preventing its biogenesis and inhibiting *trans*-Golgi-to-PM trafficking. This, in turn, leads to the initial events in the development of ALD: retention of newly synthesized proteins in the Golgi, hypertrophy, and ballooning of hepatocytes.<sup>(2)</sup>

In the liver, the function of Rab GTPases is critical for the secretion of proteins and lipids to both apical and basolateral plasma membrane (PM). We and others have recently shown that different hepatic Rab proteins, including Rab18, Rab32 and Rab7, are required to form lipid droplets and for lipophagy.<sup>(3-6)</sup> In the mouse liver, Rab5 appears to be essential for endosome biogenesis,<sup>(7)</sup> and in Hep3B hepatoma cells, Rab32 regulates lysosomal mammalian target of rapamycin trafficking.<sup>(8)</sup> Of the 70 human Rab GTPases, 20 proteins show localization in the Golgi apparatus,<sup>(9)</sup> and five proteins (Rab1, Rab6a, Rab18, Rab30, and Rab41) are required for compact and perinuclear Golgi.<sup>(8,10-12)</sup> Recently, we detected the opposite function of Rab6a in ethanol (EtOH)-treated hepatocytes. On the one hand, Rab6a recruits motor protein non-muscle myosin IIA (NMIIA) to force EtOH-induced Golgi disorganization<sup>(13)</sup>; on the other, Rab6a assists giantin dimerization required for post-ER stress or post-alcohol Golgi recovery.<sup>(14,15)</sup>

A variety of independent studies have shown that Rab3D localizes in cytoplasm and Golgi; specifically,

in rat intestinal goblet cells and in rat hepatocytes, Rab3D resides in *cis*-compartments and *trans*-compartments of Golgi and in close vicinity to the COPI vesicles.<sup>(16,17)</sup> Growing evidence indicates that the function of Rab3D is strongly linked to exocytosis. This GTPase may translocate from the cytoplasm to the *trans*-Golgi vesicles during the secretion of proteins, but is not associated with late endosomal or lysosomal compartments.<sup>(18,19)</sup> Additionally, Rab3D was detected in vesicles with the polymeric immunoglobulin A (IgA) receptor, suggesting that Rab3D may regulate transcytosis.<sup>(20)</sup> Moreover, in the *trans*-Golgi, Rab3D is essential for secretory granule maturation and size maintenance.<sup>(21,22)</sup> Furthermore, the function of Rab3D is tightly linked to the actomyosin system in PC12 cells (rat pheochromocytoma 12 cells), alveolar epithelial cells, and osteoclasts, suggesting that Rab3D may interact with various motor proteins, tethering them to the Golgi.<sup>(23-25)</sup> Despite unequivocal evidence of close relationships between Rab3D and Golgi, the precise role of this link in liver function is still unknown. Our study aims to fill this knowledge gap.

To examine the effect of Rab3D on hepatic protein trafficking, we have used the hepatic asialoglycoprotein receptor (ASGP-R). The function of ASGP-R is to remove asialoglycoproteins containing terminal galactose or N-acetylgalactosamine from circulation.<sup>(26)</sup> ASGP-R is synthesized in the rough endoplasmic

DOI 10.1002/hep4.1811

Potential conflict of interest: Nothing to report.

## ARTICLE INFORMATION:

From the <sup>1</sup>Department of Research Service, Omaha Western Iowa Health Care System, VA Service, Omaha, NE, USA; <sup>2</sup>Department of Internal Medicine, University of Nebraska Medical Center, Omaha, NE, USA; <sup>3</sup>Department of Biochemistry and Molecular Biology, University of Nebraska Medical Center, Omaha, NE, USA; <sup>4</sup>The Fred and Pamela Buffett Cancer Center, Omaha, NE, USA; <sup>5</sup>Department of Pathology and Microbiology, University of Nebraska Medical Center, Omaha, NE, USA.

## ADDRESS CORRESPONDENCE AND REPRINT REQUESTS TO:

Armen Petrosyan, M.D., Ph.D.  
Department of Biochemistry and Molecular Biology  
University of Nebraska Medical Center  
505 S 45th street  
Fred and Pamela Buffett Cancer Center, Room BCC 6.12.319  
Omaha, NE 68198-5870, USA  
E-mail: apetrosyan@unmc.edu  
Tel.: +1-402-559-1394  
or

Carol Casey, Ph.D.  
Department of Internal Medicine  
University of Nebraska Medical Center  
Omaha VA Medical Center  
4101 Woolworth Ave  
Omaha, NE 68105, USA  
Email: ccasey@unmc.edu  
Tel.: +1-402-995-3737

reticulum (ER), transported to the Golgi, and finally targeted to the plasma membrane (PM). Following ligand binding, ASGP-R is endocytosed and delivered to early endosomes. The ligand-ASGP-R complex is then transported to recycling endosomes, where they dissociate. Then, the ligand is transferred to the lysosome for degradation, and unoccupied ASGP-Rs are either returned to the cell surface or degraded. We have had a long-standing interest in endocytosis by ASGP-R and identified multiple EtOH-induced alterations, including impaired receptor recycling and protein assembly into the PM.<sup>(2,27,28)</sup> We found that, in addition to altering endocytosis and causing Golgi disorganization, EtOH impairs ASGP-R trafficking within the Golgi. This results in incomplete glycosylation of ASGP-R and is due to retardation of intra-Golgi trafficking and redistribution of some critical Golgi resident enzymes to the ER.<sup>(29,30)</sup>

Typically, ASGP-R is expressed on the sinusoidal membrane of hepatocytes; however, in patients with cirrhosis, the receptor is also redistributed to the apical surface<sup>(31)</sup> and potentially secreted into the bloodstream as a soluble variant of ASGP-R (s-ASGP-R).<sup>(32)</sup> Importantly, s-ASGP-Rs binds to the surface of erythrocytes, causing dose-dependent agglutination and hemolysis, especially in patients with blood group A1. This is indicative of an unfavorable prognosis, but the mechanism of ASGP-R secretion is enigmatic. In addition, defective ASGP-R and its deficiency at the PM have apparent effects on several physiological processes, including decreased clearance of apoptotic bodies, increased inflammation in the liver due to activation of nonparenchymal cells (Kupffer cells), and potential involvement in alcohol-increased liver metastases from colorectal cancer.<sup>(33-35)</sup> In this study we showed that in animal and human models of ALD, alcohol-induced down-regulation of Rab3D and Golgi remodeling plays a critical role in abnormal distribution of ASGP-R.

## Animals and Methods

VA-13 cells (mouse ADH1-transfected HepG2 cells) were obtained from Dr. Dahn Clemens (Nebraska Western Iowa Health Care System).<sup>(36)</sup> For EtOH-treated cells, regular culture media was removed 24 hours after seeding (at ~75% confluency), and culture media was supplemented with 35 mM EtOH

for an additional 96 hours. The culture medium was changed every 12 hours to hold the EtOH concentration constant. Control cells were seeded, and media was changed on the same schedule as the EtOH cells, and an appropriate volume of medium was supplemented to these cells to balance the caloric content of the EtOH. WIF-B cells were obtained from Dr. Pamela Tuma (The Catholic University of America, Washington, DC) and were grown at 37°C in F-12 media containing 3.5% heat-inactivated Fetalplex in a 7% CO<sub>2</sub> atmosphere as described previously.<sup>(37)</sup> Cells were seeded on sterilized glass coverslips or directly in tissue culture dishes and cultured for 6 days to obtain a maximal-polarized phenotype before EtOH treatment (50 mM). Primary rat and mice hepatocytes from control and EtOH-fed animals were prepared from the C57BL/6 mice (Jackson Laboratory, Bar Harbor, ME) and male Wistar rats (Charles River Laboratories, Wilmington, MA). Rab3D KO mice are available to us from Dr. Jahn Reinhard (Max Planck Institute for Biophysical Chemistry, Göttingen, Germany).<sup>(21)</sup> We generated homozygous mice by crossing Rab3D KO/WT heterozygous mice at the University of Nebraska Medical Center (UNMC). All animals were initially fed a basic Purina chow diet while acclimating to the surroundings during the first 3 days. The animals were then paired by weight and split into the control-fed or EtOH-fed groups and maintained for 5-8 weeks. The EtOH-containing Lieber-DeCarli diet consisted of 35% fat, 18% protein, 11% carbohydrates, and 36% EtOH (Dyets Inc., Bethlehem, PA). The control diet was identical to the EtOH diet except for the isocaloric substitution of carbohydrates in the place of the EtOH. This protocol was approved by the Institutional Animal Care and Use Committee of the Department of Veterans Affairs, Nebraska Western Iowa Health Care System, and UNMC. A modified collagenase perfusion technique was used to isolate hepatocytes from the livers of control and EtOH-fed rats used and described previously by the Casey laboratory.<sup>(28)</sup>

The details of other methods and materials are described in the Supporting Information. These include antibodies and reagents; small interfering RNA (siRNA) transfection; immunohistochemistry (IHC); confocal immunofluorescence (IF) microscopy; three-dimensional (3D) structured illumination microscopy and image analysis; plasma membrane isolation, endoglycosidase H (Endo H), and sialidase

digestion; isolation of microsomal fraction; proteomics analysis of electrophoretically separated proteins; *in situ* proximity ligation assay; patient-derived tissue samples; and quantification and statistical analysis.

## Results

### DOWN-REGULATION OF Rab3D IS ASSOCIATED WITH ALTERATION OF GOLGI MORPHOLOGY

Previously, in EtOH-fed rats, we found a significantly decreased total liver content of Rab3D and reduced expression of Rab3D mRNA.<sup>(4,38)</sup> To evaluate this observation in other hepatocyte systems, we measured the expression of Rab3D in VA-13 and WIF-B cells, the widely used cellular models of ALD.<sup>(36,37)</sup> In both cells, EtOH treatment reduced the content of Rab3D (Fig. 1A,B). Importantly, Rab3D demonstrated an intense perinuclear localization, and EtOH-induced Golgi disorganization<sup>(2)</sup> was associated with an apparent reduction in its IF intensity (Fig. 1C,D). Contrary to Rab3D, other Rab3 isomers (A, B, and C) were detected in both Golgi and cytoplasm, and their protein level did not change significantly in either EtOH-treated VA-13 cells or hepatocytes from alcohol-fed rats (Supporting Fig. S1A-C). To validate that Rab3D reduction is associated with an alcohol-induced liver injury, we performed Rab3D IHC on the liver tissue samples obtained from donors with and without a history of alcohol use and patients with alcoholic steatohepatitis (ASH) (Supporting Table S1). No difference was present in the intensity of Rab3D between the donor groups; however, a robust decrease of Rab3D IHC signal was detected in patients with ASH compared with either group of donors (Fig. 1E,F). Next, we found that the level of Rab3D was also reduced in the liver tissue lysate samples obtained from patients with alcohol-associated cirrhosis compared with the representatives from non-alcohol-associated donors (Fig. 1G,H). We believe that these data are important from the clinical point of view: The decrease in the Rab3D could serve as a prognostic factor for the manifestation of ALD.

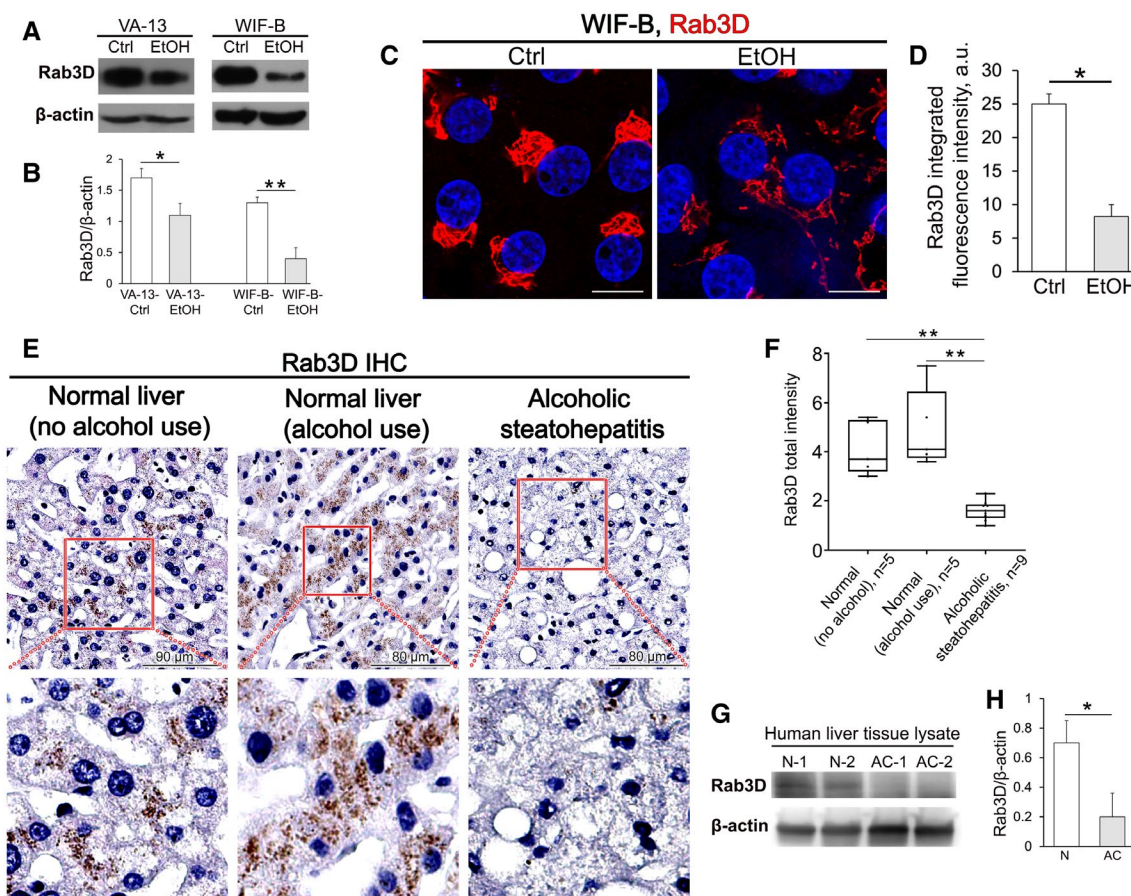
It has been shown that several Rab proteins are critical for the maintenance of compact Golgi.<sup>(10-12)</sup> Therefore, we examined whether the lack of Rab3D

may affect the structural organization of Golgi. In VA-13 cells, siRNA-mediated knockdown (KD) of Rab3D does not change the expression of other Rab3 GTPases, indicating that the compensatory mechanisms for the composition of Rab3 isoforms do not occur when Rab3D is decreased (Fig. 2A,B). However, we noticed that depletion of Rab3D changes the organization of *trans*-Golgi, resulting in enlarged Golgi (Fig. 2C,D). This was further confirmed by transmission electron microscopy (EM), showing that Rab3D KD causes enlargement of Golgi cisternal membranes counted based on their average luminal width (Fig. 2E,F for Kolmogorov–Smirnov plots (Fig. 2G). Similarly, no significant changes in expression of the other three Rab3 isoforms were observed in hepatocytes from Rab3D knockout (KO) mice (Fig. 2H,I), and the morphology of Golgi in Rab3D KO hepatocytes appeared enlarged compared with the wild type (WT) (Fig. 2J). Quantification of the Golgi area indicates that Rab3D maintains normal Golgi morphology (Fig. 2K).

To examine the precise intra-Golgi distribution of Rab3D, we used the structured illumination superresolution microscopy (SIM), which allowed us to achieve two-color 3D imaging at about 110-nm resolution. IF data were analyzed by Pearson's colocalization coefficient to quantify the association of Rab3D with different Golgi markers: TGN46 (*trans*-Golgi), giantin (*medial*-Golgi), and GM130 (*cis*-Golgi). In control WIF-B cells and rat hepatocytes, Rab3D predominantly colocalized with TGN46 rather than giantin or GM130, suggesting that Rab3D resides primarily within *trans*-Golgi (Fig. 3A-G, left panels). However, in EtOH-treated WIF-B cells and hepatocytes from alcohol-fed rats, Rab3D predominantly colocalized with GM130 and giantin, suggesting a shift of Rab3D residence to *cis-medial*-Golgi (Fig. 3A-G, right panels). Thus, we concluded that EtOH-induced Golgi disorganization<sup>(2)</sup> was associated with impaired intra-Golgi trafficking of Rab3D.

### Rab3D AND COPI ARE INTERCONNECTED

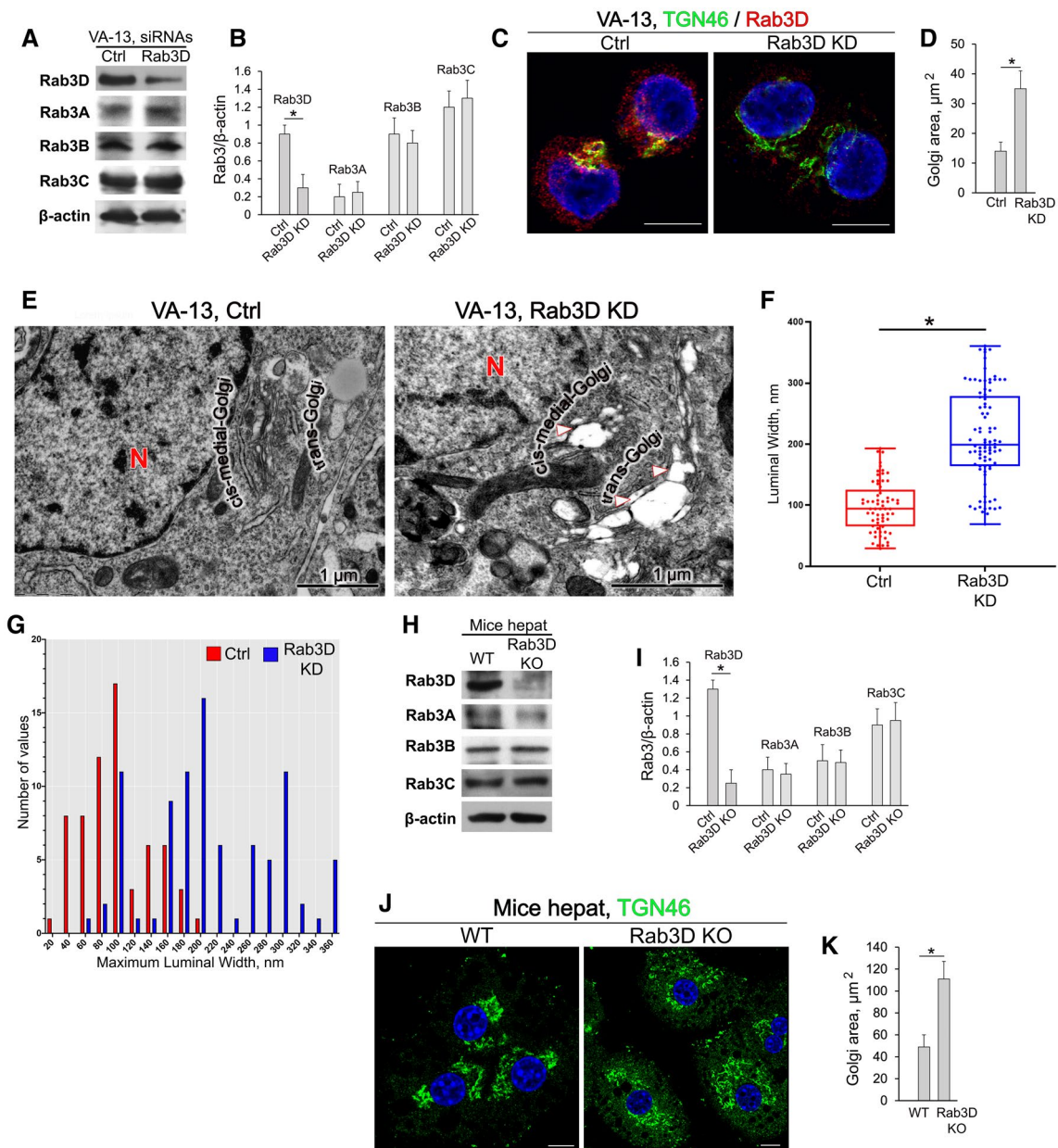
Previously, we found that EtOH blocks activation of Arf1 (ADP-ribosylation factor 1), a key small GTPase that initiates COPI vesicle formation in Golgi; subsequent down-regulation of COPI results in redistribution of key Golgi-resident N-glycosylation enzymes



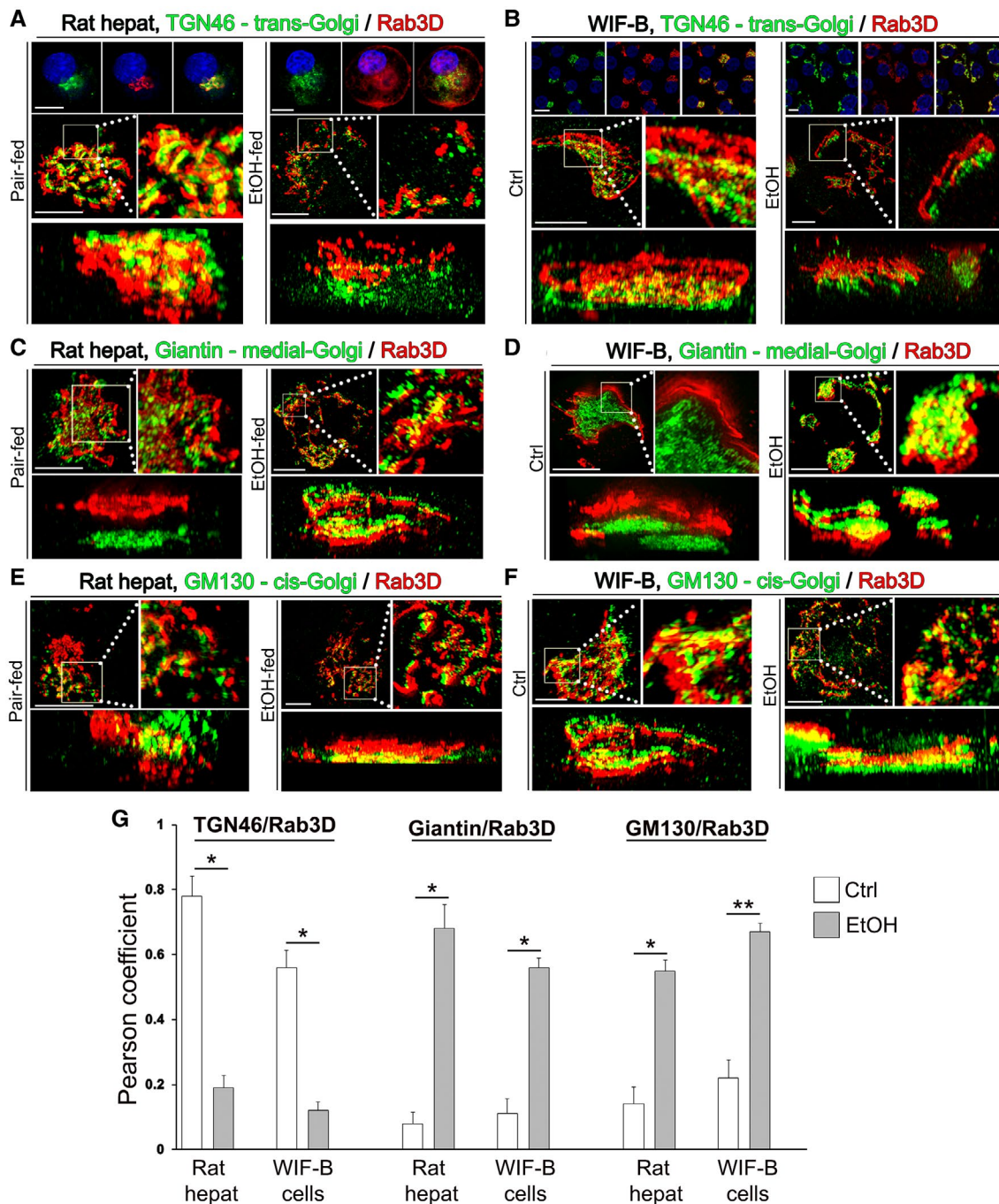
**FIG. 1.** Chronic alcohol administration reduces the level of Rab3D. (A) Rab3D western blot of the lysate of VA-13 cells treated with 35 mM EtOH for 96 hours and WIF-B cells treated with 50 mM EtOH for 96 hours;  $\beta$ -actin is a loading control. (B) Densitometric analysis of ratio Rab3D/ $\beta$ -actin based on the data from three repeats. \* $P < 0.001$ , \*\* $P < 0.01$ ,  $t$  test, mean  $\pm$  SD. (C) Representative IF images of Rab3D (red) in EtOH-treated WIF-B cells. Nuclei in blue (DAPI); bars, 10  $\mu$ m. (D) Quantification of Rab3D IF intensity from cells presented in (C);  $n = 90$  cells for each sample from three independent experiments, \* $P < 0.001$ ,  $t$  test, mean  $\pm$  SD. (E) Representative images of Rab3D IHC (brown) in the human liver tissue sections from non-alcohol-associated donors, donors consuming alcohol, and patients with ASH. Red squares indicate the area enlarged below. Nuclei were stained with hematoxylin. (F) Quantification of Rab3D intensity from the samples presented in (E); \*\* $P < 0.01$ , unpaired  $t$  test between the donor groups and unpaired Welch's  $t$  test between the donors and patients with ASH; medians (min-max). The details of quantification are described in the Supporting Methods. (G) Rab3D western blot of the liver tissue lysate samples obtained from the donors (N) and patients with alcohol-associated cirrhosis (AC). (H) Densitometric analysis of the ratio Rab3D/ $\beta$ -actin from 5 healthy individuals and 5 patients with cirrhosis,  $t$  test, mean  $\pm$  SD. Abbreviations: AC, alcohol-associated cirrhosis; Ctrl, control; DAPI, 4',6-diamidino-2-phenylindole; N, normal control.

and abnormal glycosylation of ASGP-R.<sup>(39)</sup> The data presented leads us to assume that trafficking and distribution of Rab3D in Golgi membranes are mediated by COPI vesicles. To check this possibility, we performed a mass-spectrometric proteomic analysis of the strong protein bands eluted from sodium dodecyl sulfate-polyacrylamide gel electrophoresis of immunoprecipitated Rab3D (Fig. 4A). Among other Golgi-associated proteins, *trans*-Golgi golgin p230/golgin-245, cyto-keratin 1, and NMIIB, we detected COPI subunit

$\beta$ -COP. To evaluate the physical closeness of Rab3D and COPI in VA-13 cells, we performed a quantitative *in situ* proximity ligation assay (PLA), which can detect protein-protein interaction by the visualization of red fluorescence emanating from the proximity (below 40 nm) of these two proteins. During growth, VA-13 cells form cluster-like colonies. So, we performed Z-stacks scanning for a more accurate count followed by 3D rendering with PLA spots reconstruction (for details, see the Supporting Methods). As shown in



**FIG. 2.** Depletion of Rab3D affects Golgi morphology. (A) Rab3D, A, B, and C western blot of the lysates of control and Rab3D KD VA-13 cells. (B) Densitometric analysis of ratio Rab3/ $\beta$ -actin for the indicated Rab3 proteins from three repeats of the experiment presented in (A),  $*P < 0.001$ ,  $t$  test, mean  $\pm$  SD. (C) Representative IF images of TGN46 (green) and Rab3D (red) in control and EtOH-treated VA-13 cells; bars, 10  $\mu$ m. (D) Quantification of Golgi area of the cells presented in (C). Area of the Golgi was evaluated using ImageJ;  $n = 90$  cells from three independent experiments;  $*P < 0.001$ ,  $t$  test, mean  $\pm$  SD. (E) Representative EM micrographs of VA-13 cells treated with scramble and Rab3D siRNAs. *Cis-medial* and *trans*-Golgi are highlighted. Arrowheads indicate enlarged Golgi cisternae. (F) Quantification summarizing the maximum luminal width of *trans*-Golgi cisternal elements. Data were tested for normality using the Kolmogorov Smirnov test,  $P < 0.0001$  ( $n = 65$  for control and  $n = 89$  for Rab3D KD cells). (G) Frequency distribution histograms for maximum cisternal luminal width analysis for both control and Rab3D KD samples. (H) Rab3D, A, B, and C western blot of the lysates of hepatocytes from WT and Rab3D KO mice. (I) Densitometric analysis of ratio Rab3/ $\beta$ -actin for the indicated Rab3 proteins from three repeats of the experiment presented in (H),  $*P < 0.001$ ,  $t$  test, mean  $\pm$  SD. (J) Representative IF images of TGN46 (green) in hepatocytes from WT and Rab3D KO mice; bars, 5  $\mu$ m. (K) Quantification of Golgi area of the cells presented in (J);  $n = 90$  from three independent experiments,  $*P < 0.001$ ,  $t$  test, mean  $\pm$  SD. Abbreviation: N, nucleus.



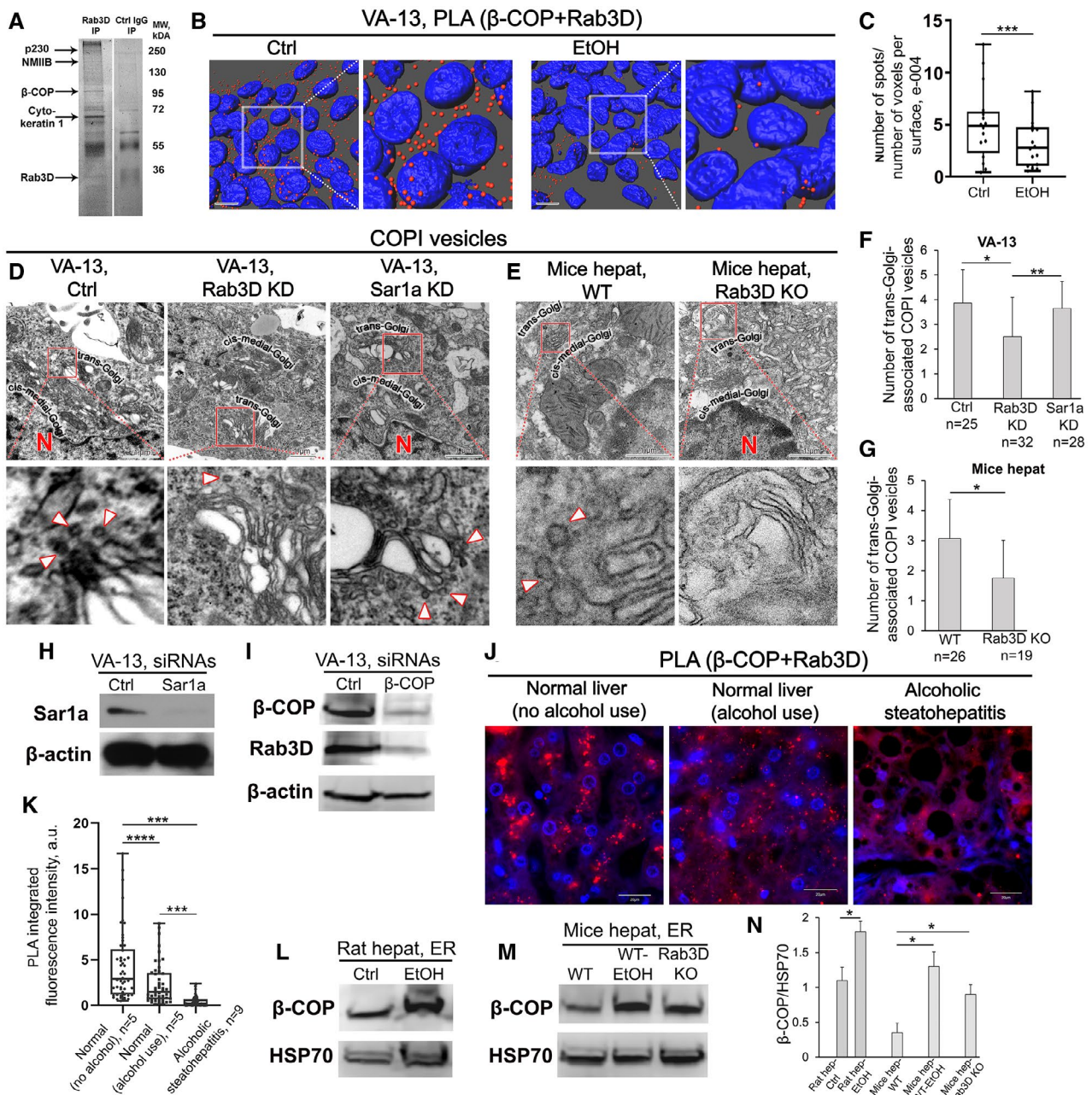
**FIG. 3.** EtOH alters the distribution of Rab3D in Golgi. 3D-SIM projection of Golgi in hepatocytes from pair-fed or EtOH-fed rats and WIF-B cells (control or treated with EtOH). Cells are stained with Rab3D (red) and different Golgi markers (green): *trans*-Golgi TGN46 (A,B, representative cells presented on the top panel); *medial*-Golgi, giantin (C,D), and *cis*-Golgi, GM130 (E,F). White boxes are enlarged at the right. Bars: top panel, 5  $\mu$ m for rat hepatocytes and 10  $\mu$ m for WIF-B cells; 3D SIM images, 500 nm. (G) Quantification of colocalization for indicated proteins from the images presented in (A)-(F); n = 10 SIM images for each series of experiments, \* $P$  < 0.001, \*\* $P$  < 0.01,  $t$  test. Data are presented as mean  $\pm$  SD.

Fig. 4B and Supporting movies 1 and 2, the number of spots was significantly reduced in EtOH-treated cells, which was statistically validated (Fig. 4C). In the control

PLA experiment, VA-13 cells were incubated separately with either  $\beta$ -COP or Rab3D Abs; however, no visible PLA signal was detected (Supporting Fig. S2A,B).

These data can be interpreted in two ways. On the one hand, EtOH reduces the number of both COPI vesicles and Rab3D, inevitably reducing the PLA-detected cooperation of  $\beta$ -COP and Rab3D. On the other hand, one could assume that Rab3D is required for the formation of COPI. In this case, EtOH-induced down-regulation of Rab3D in *trans*-Golgi (Fig. 3) can also contribute to COPI deficiency. If so, cells lacking Rab3D should have fewer COPI-coated vesicles budding from the rims of the *trans*-Golgi cisternae. To verify this in VA-13 cells, we counted the

number of *trans*-Golgi-associated COPI vesicles by EM. As anticipated, in Rab3D KD cells, the number of these vesicles was significantly reduced compared with the control (Fig. 4D,F). However, two interesting aspects must be considered. First, chronic EtOH administration blocks formation of COPII vesicles and induces ER stress.<sup>(2,40)</sup> Second, depletion of Sar1a (the GTPase that initiated COPII vesicles assembly) induces ER stress<sup>(41)</sup>; and vice versa, ER stress down-regulates COPII.<sup>(42)</sup> Given that ER stress and Golgi stress are reciprocally coordinated,<sup>(43)</sup> we speculated





**FIG. 4.** Association of Rab3D and COPI vesicles. (A) Coomassie brilliant blue stain of proteins co-immunoprecipitated with Rab3D. Control immunoglobulin G immunoprecipitation is shown next to Rab3D IP. Arrows indicate proteins identified by mass spectrometry. (B) Representative 3D-reconstructed images of PLA to detect  $\beta$ -COP and Rab3D proximity in control and EtOH-treated VA-13 cells; blue, nucleus, DAPI; bars, 10  $\mu$ m. White boxes highlight the area enlarged at the right. (C) Quantification of the PLA signal was performed using the following ratio: number of spots/total number of voxels in the nuclear surface. The details of quantification are described in the Supporting Methods.  $***P < 0.05$ , Welch's one-tailed *t* test. Data are presented as medians (min-max) from two independent experiments;  $n = 549$  cells for control and  $n = 908$  for EtOH-treated cells. (D,E) Representative EM images of Golgi-associated COPI vesicles in VA-13 cells (control, Rab3D KD, and Sar1a KD) (D) and hepatocytes from WT and Rab3D KO mice (E). Red squares indicate the *trans*-Golgi area enlarged below. Arrowheads indicate COPI vesicles budding from the rims of *trans*-Golgi; bars, 1  $\mu$ m. (F,G) Quantification summarizing the average number of *trans*-Golgi-associated budding vesicles in cells from (D) and (E), respectively. The results from two independent experiments are expressed as a mean  $\pm$  SD;  $n =$  the number of Golgi stacks for which vesicles were counted (listed in the figure);  $*P < 0.001$ ,  $**P < 0.01$ , *t* test. Data are presented as mean  $\pm$  SD. (H) Sar1a western blot of the lysate of VA-13 cells treated with control or Sar1a siRNAs. (I)  $\beta$ -COP and Rab3D W-B of the lysate of VA-13 cells treated with control or  $\beta$ -COP siRNAs. (J) PLA assay of human liver tissue sections; mouse anti- $\beta$ -COP and rabbit anti-Rab3D antibodies were used. All images were acquired with identical imaging parameters; bars, 20  $\mu$ m. (K) Quantification of the PLA signal from samples presented in (I).  $****P < 0.0001$ ,  $***P < 0.05$ , Kruskal-Wallis with Dunn's correction;  $n =$  number of donors/patients (listed in Supporting Table S1). Data are presented as medians (min-max). (L,M)  $\beta$ -COP western blot of the ER fraction isolated from hepatocytes of control and alcohol-fed rats (L) and hepatocytes from control and alcohol-fed WT mice and control Rab3D KO mice (M). (N) Densitometric analysis of ratio  $\beta$ -COP/HSP70 for the indicated samples from three repeats of experiments presented in (L) and (M),  $*P < 0.01$ , *t* test, mean  $\pm$  SD. Abbreviations: IgG, immunoglobulin G; IP, immunoprecipitation; N, nucleus.

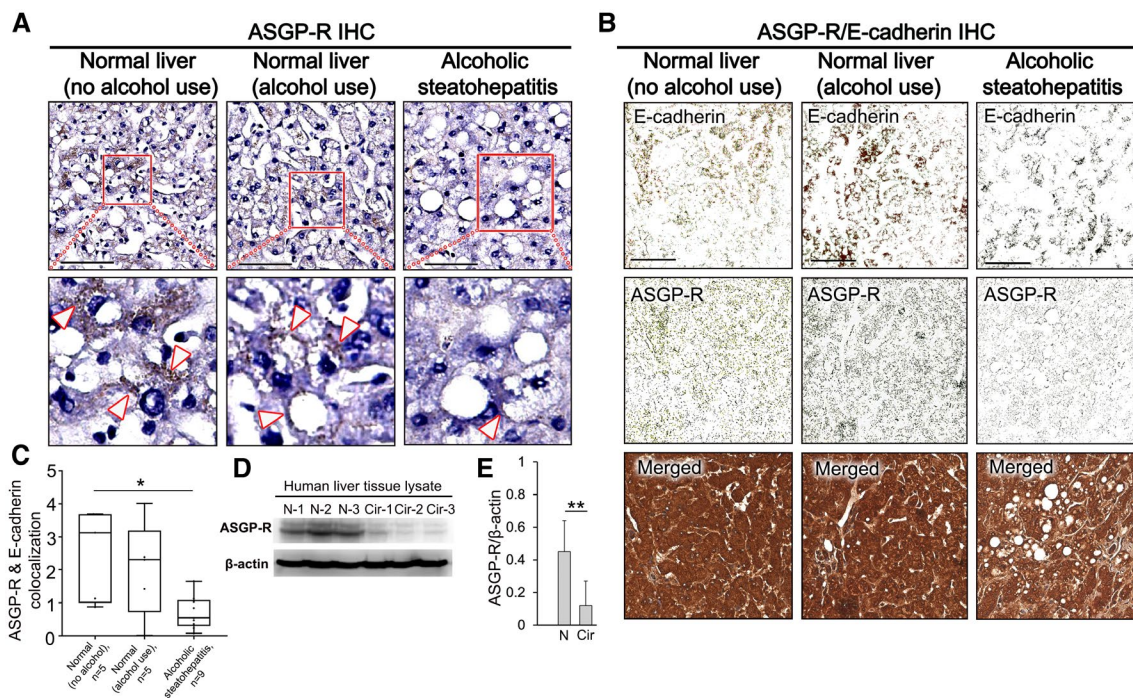


**FIG. 5.** Alcohol-associated liver disease is associated with the down-regulation of ASGP-R. (A) Representative images of ASGP-R IHC (brown) in the human liver tissue sections. Red squares indicate the area enlarged below. Arrowheads indicate the peripheral ASGP-R-specific dots. Nuclei were stained with hematoxylin. (B) ASGP-R (green) and E-cadherin (brown) IHC co-staining in the human liver tissue sections. Bars for (A) and (B) are 80  $\mu$ m. The “Convolution algorithm” of Aperio software reduces the signal of E-cadherin to get a more distinct peripheral (cell surface) signal, and then deconvoluted channels (ASGP-R and E-cadherin) were subjected to the “Colocalization algorithm” to measure ASGP-R signal on the plasma membrane. (C) Quantification of colocalization of ASGP-R with E-cadherin in the samples from (B). Unpaired Welch's *t*-test; mean (min-max),  $*P < 0.05$ . (D) ASGP-R W-B of liver tissue lysate samples obtained from normal donors and patients with cirrhosis. (E) Densitometric analysis of ratio ASGP-R/ $\beta$ -actin from 5 normal and 5 cirrhotic samples,  $**P < 0.01$ , *t* test, mean  $\pm$  SD. Abbreviations: Cir, patients with cirrhosis; N, normal donors.

that the EtOH-induced impairment of COPI could be partially ascribed to the development of ER stress and lack of COPII vesiculation. However, quantification of COPI vesicles in Sar1a-depleted VA-13 cells did not confirm this possibility: The number of COPI linked to the *trans*-Golgi was identical to the control (Fig. 4D,F,H). Importantly, in VA-13 cells, depletion of  $\beta$ -COP results in a reduction of Rab3D protein level (Fig. 4I). Taken together, this reinforces the idea that the function of Rab3D is tightly linked to COPI vesicles reconstituted from Golgi membranes. Indeed, in hepatocytes from Rab3D KO mice, the number of *trans*-Golgi associated COPI was significantly reduced compared with those from WT mice (Fig. 4E,G).

Next, using PLA, we evaluated the closeness of Rab3D and  $\beta$ -COP in human liver tissue sections from donors with and without a history of alcohol consumption and patients with ASH. Similar to VA-13 cells, the control PLA experiment with separate incubation of either  $\beta$ -COP or Rab3D Abs reveals little if any PLA signal (Supporting Fig. S2C,D). Interestingly, in persons drinking alcohol but without steatohepatitis, the co-association of Rab3D/ $\beta$ -COP was reduced compared with the donors who do not consume alcohol (Fig. 4J,K). However, as shown previously, these groups did not differ in their Rab3D expression (Fig. 1D). In the ASH patient group, the Rab3D/ $\beta$ -COP PLA intensity was significantly decreased compared with the donor groups. These data indicate that alteration of Rab3D and COPI interaction precedes liver injury, and reduction of Rab3D may contribute to the subsequent manifestation of ALD. Notably, in alcohol-fed rats, the level of ER-residing  $\beta$ -COP was enhanced, confirming that incorporation of  $\beta$ -COP into COPI complex in the Golgi is altered (Fig. 4L,N). Similar results were obtained from alcohol-fed mice; moreover, the level of  $\beta$ -COP in the ER fraction from Rab3D KO mice was also elevated compared with the WT group (Fig. 4M,N).

### Rab3D PLAYS A CRITICAL ROLE IN ALCOHOL-INDUCED IMPAIRMENT OF ASGP-R DISTRIBUTION

Next, we evaluated PM's ASGP-R signal in clinical samples from patients with ASH or donors with and without habitual alcohol consumption. First, we

examined ASGP-R distribution by IHC (Fig. 5A). Predictably, in the donor groups, most IHC signal was detected in the cytoplasm, but we were also able to detect a strong PM expression of ASGP-R (Fig. 5A, red arrowheads). The overall intensity of the IHC signal was lower in the tissue from patients with ASH; therefore, to precisely quantify the ASGP-R signal on the PM, we co-stained these sections with both ASGP-R and PM marker E-cadherin (Fig. 5B). We found no difference in ASGP-R/E-cadherin colocalization between the donor groups; however, a significant reduction of colocalization was found in patients with ASH patients compared to donors without a history of alcohol use (Fig. 5C). Finally, we found that the total level of ASGP-R in liver tissue lysates from patients with alcohol-associated cirrhosis was reduced compared with control samples (Fig. 5D,E).

The data presented here clearly demonstrate that, despite EtOH-induced Golgi fragmentation, abnormally glycosylated ASGP-R can still reach the cell surface,<sup>(39)</sup> but the mechanism of their trafficking remains unknown. An early publication from our lab indicates that these ASGP-R molecules have a reduced binding capacity.<sup>(28)</sup> This is logical, as only fully glycosylated ASGP-R can bind effectively to asialoglycoproteins.<sup>(44)</sup> Here, we aimed to evaluate whether Rab3D deficiency affects ASGP-R distribution and glycosylation. We performed ASGP-R immunogold EM in hepatocytes isolated from WT and Rab3D KO mice. In WT cells, ASGP-R was widely presented in all organelles representing different steps of this protein trafficking: rough ER, Golgi, PM, and endosomes (Fig. 6A). Notably, the distribution of ASGP-R in *cis-medial*-Golgi and *trans*-Golgi was almost identical (Fig. 6A, *Golgi* panel, insets a and b). Compared with WT cells, Rab3D KO hepatocytes demonstrate a reduced amount of ASGP-R in Golgi and at the PM (Fig. 6C,D). Notably, most Golgi-specific dots were detected in the *cis-medial*-Golgi compartments and not *trans*-Golgi (Fig. 6B, *Golgi* panel, insets a and b). This is indicative of stalled intra-Golgi trafficking. Also, the number of ASGP-R dots in endosomes was decreased almost 3-fold (Fig. 6E), indicating that the pool of fully glycosylated ASGP-R is significantly reduced in Rab3D-KO hepatocytes. However, the amount of ASGP-R in the ER was enhanced (Fig. 6F), suggesting retardation of ER-to-Golgi trafficking. Finally, ASGP-R was detected in the cytoplasm of both cell types with no

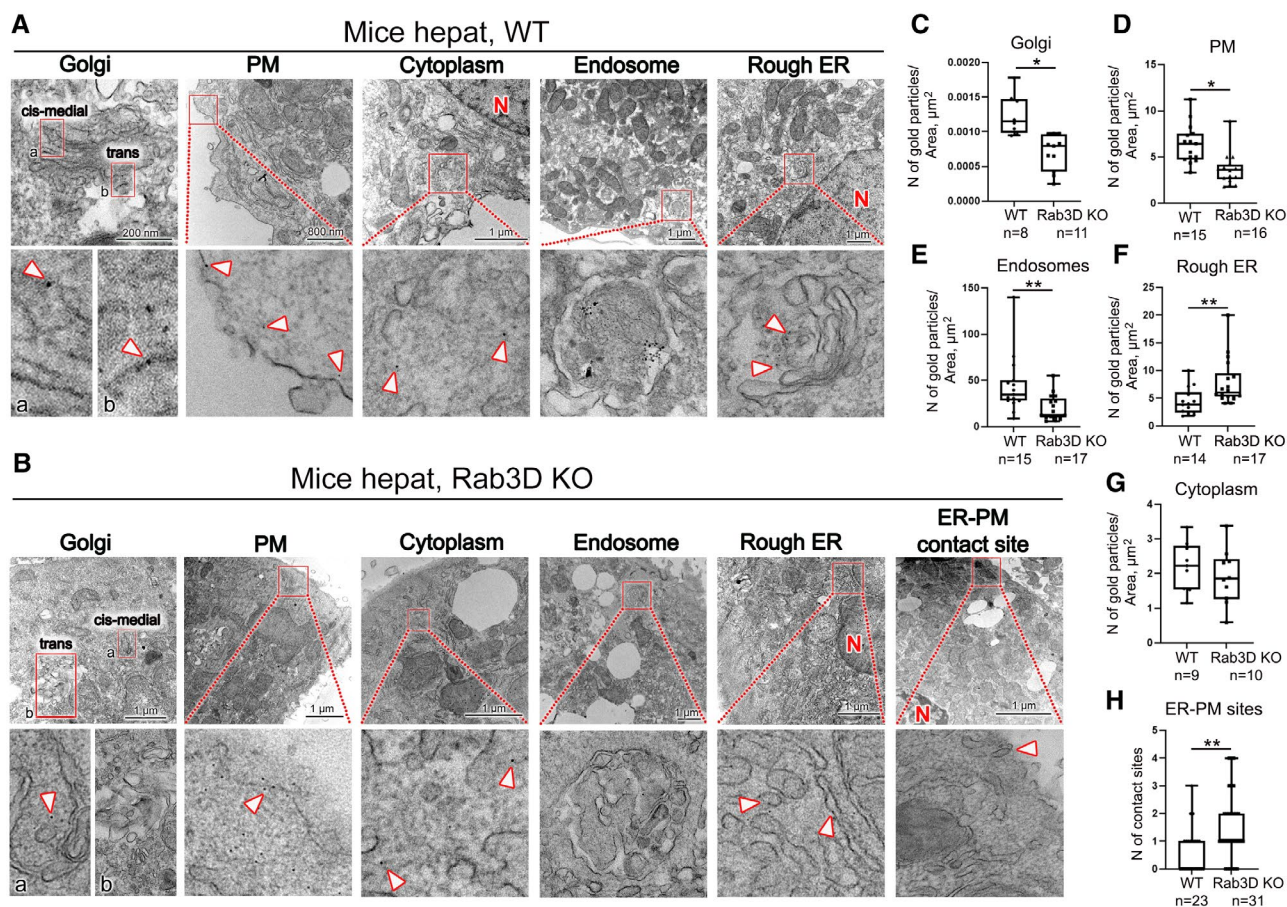


**FIG. 6.** Rab3D depletion significantly changes ASGP-R distribution. (A,B) Representative pre-embedding immunogold EM analyses of ASGP-R in hepatocytes from WT and Rab3D KO mice. Red squares indicate the organelle area enlarged below. Arrows indicate the ASGP-R specific immunogold particles and ER-PM contact site. The insets *a* and *b* in the Golgi panel represent *cis-medial*- and *trans*-Golgi membranes, accordingly. (C-G) ASGP-R distribution in different organelles and cytoplasm is counted as a ratio of the number of gold particles to the area of organelle (in squared micrometers). Mean (min-max) and unpaired *t* test were used for Golgi, PM, and cytoplasm; median (min-max) and Mann-Whitney U test were used for endosomes and rough ER. (H) Quantification of ER-PM contact sites in WT and Rab3D KO hepatocytes; mean  $\pm$  SD, unpaired *t* test, mean (min-max). \**P* < 0.001 and \*\**P* < 0.01 for all graphs. Abbreviation: N, nucleus.

difference (Fig. 6G). Therefore, in Rab3D-KO cells, ASGP-R was detected at PM despite impaired trafficking, implying that this receptor likely can reach the cell surface by an alternative trafficking pathway, bypassing Golgi membranes. Intriguingly, in KO hepatocytes, we were able to detect ER-PM contact sites whose number were significantly higher than that in WT cells (Fig. 6B, ER-PM contact site panel, and 6H).

Accumulation of ASGP-R immunogold spots in the ER of Rab3D-KO hepatocytes suggests that lack of Rab3D alone may induce ER stress and accelerate alcohol-induced unfolded protein response (UPR).

Here, in WT and Rab3D-KO mice, we monitored the expression of ER stress chaperone GRP78 and activation of different branches of UPR, activating transcription factor 6 (ATF6), inositol-requiring enzyme 1 (IRE1), and endoplasmic reticulum kinase (PERK). We found that in hepatocytes from alcohol-fed WT mice, expression of GRP78 and cleaved ATF6 was predictably enhanced compared with control (Supporting Fig. S3A-C). Importantly, control Rab3D-KO mice also demonstrate an increase in GRP78 levels and cleaved ATF6, which was more prominent when mice were fed with alcohol (Supporting Fig. S3A-C). Similarly, activation of IRE1 and PERK (based on

the content of their phospho-form) was also detected not only in alcohol-fed WT mice, but also in control Rab3D-KO mice; however, the levels of phospho-PERK and phospho-IRE1 were not different between control and alcohol-fed Rab3D-KO mice (Supporting Fig. S3D-G). Next, we detected a rise of ASGP-R content in the ER fraction of control Rab3D-KO mice compared with control WT mice (Supporting Fig. S3H,I), echoing the results from EM (Fig. 6). In the ER fraction, we also observed accumulation of other hepatic proteins: transferrin (Tf) and polymeric IgA receptor (pIgR) (Supporting Fig. S3H,I). Therefore, depletion of Rab3D KO and subsequent ER stress may affect multiple pathways of hepatic protein trafficking: endocytosis (ASGP-R), secretion (Tf), and transcytosis (pIgR). Considering this, it appears that Rab3D deficiency enhances the damaging effect of EtOH.

However, when Rab3D-KO mice were administered the Lieber-DeCarli diet for 8 weeks, only 35% of the mice survived. Using perilipin-1 staining of liver tissue sections, we monitored the distribution of lipid droplets in control and EtOH-fed WT and Rab3D KO mice. EtOH-fed WT mice predictably demonstrated fat accumulation, but the same phenomenon was observed in the liver of control Rab3D-KO mice (Supporting Fig. S4A,B). Moreover, Rab3D-KO mice consuming alcohol demonstrate more intense staining of perilipin-1 than their WT counterparts (Supporting Fig. S4A,B). Next, an increased expression of cleaved caspase-3 was detected in hepatocytes from alcohol-fed Rab3D-KO mice compared with the alcohol-fed WT mice (Supporting Fig. S3J,K). However, some of the alcohol-fed Rab3D-KO mice did not demonstrate a significant increase in liver injury markers (data were not quantified due to the low number of animals compared with a control group). Given the whole-body Rab3D KO, we may speculate that alcohol-associated mortality of these mice is more complex and could be linked to the damaging effect of EtOH on other organs.

## ALTERNATIVE TRAFFICKING OF ASGP-R BYPASSES THE GOLGI

Based on the results presented previously, we can conclude that depletion of Rab3D partially mimics the effect of EtOH on Golgi morphology and distribution of ASGP-R. Similar to Rab3D KO

hepatocytes, in EtOH-treated VA-13 cells, we were able to detect by EM additional ER-PM contact sites (Fig. 7A,B). To confirm that ASGP-R can be expressed at PM through these sites, we performed high-resolution SIM imaging of VA-13 cells, co-staining ASGP-R with PM marker E-cadherin and ER marker calreticulin (Fig. 7C; Supporting Movies S3 and S4). Then, using the 3D reconstruction of images in all projections, we rigorously counted the number of triple-stained merged spots. Quantification indicated that EtOH-treated cells have an increased number of ASGP-R spots merged with ER and PM (Fig. 7D). To determine whether ASGP-R passes through the Golgi en route to the cell surface, we examined the sensitivity of the PM's ASGP-R (PM-ASGP-R) to recombinant Endo H and sialidase. It is known that Endo H cleaves high mannose and hybrid glycans, but complex glycans (those with complete glycosylation in the Golgi) are resistant to hydrolysis. Conversely, sialidase-sensitive proteins supposedly transport through the Golgi and undergo sialylation. Therefore, if PM-ASGP-R is Endo H-sensitive and sialidase-resistant, it likely circumvented the Golgi. In Rab3D KO hepatocytes, PM-ASGP-R was sensitive to Endo H, displaying the cleaved protein fragment, while the sensitivity in WT cells was moderate (Fig. 7E, top panel, asterisk). PM-ASGP-R from WT cells was sialidase-sensitive, but minimal sensitivity was detected in the Rab3D KO sample (Fig. 7E, lower panel, asterisk).

Furthermore, we found that PM-ASGP-R1 isolated from control rat hepatocytes demonstrate two bands: approximately 35 kDa and 25 kDa. The latter is sensitive to sialidase (Fig. 7F, control, asterisk). Notably, in EtOH-fed rats, the PM-ASGP-R1 35-kDa band is converted to the 70-kDa form (presumably, dimer), whereas the 25-kDa band shows a weak response toward sialidase digestion (Fig. 7F, EtOH panel). Overall, these data support the claim that in Rab3D-deficient or EtOH-treated hepatocytes, the PM-ER contacts serve as an alternative delivery avenue for cell surface proteins. In a proof-of-principle experiment, we treated VA-13 cells with EtOH and transfected them with hRab3D complementary DNA, thus overexpressing exogenous Rab3D. As shown in Fig. 7G,H, transfection of Rab3D plasmid rescued Rab3D levels after EtOH treatment and maintained the amount of ASGP-R at the cell surface identical to control.

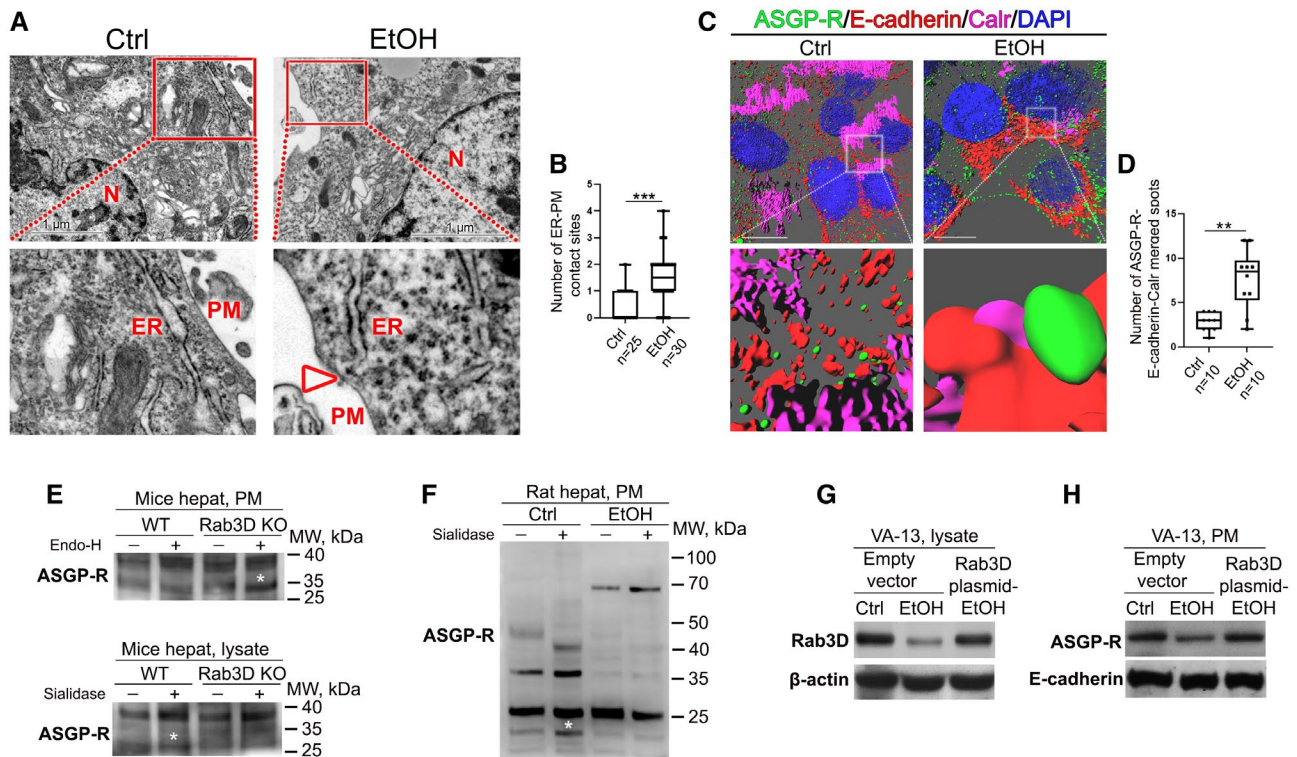


**FIG. 7.** ASGP-R can reach the cell surface—bypassing Golgi. (A) Representative EM images of control and EtOH-treated VA-13 cells. Red squares indicate the area enlarged below. Arrowhead indicates direct ER-PM contact site. (B) Quantification of ER-PM connections in cells from (A); median (min-max) and Mann-Whitney U test,  $***P < 0.001$ . (C) Representative images of 3D-SIM projection from control and EtOH-treated VA-13 cells. Cells are stained with ASGP-R (green), E-cadherin (red), and calreticulin (magenta). White squares represent the area of merged ASGP-R/E-cadherin/calreticulin spots magnified through 3D projection and presented below; bars, 10  $\mu\text{m}$ . (D) Quantification of the number of merged green/red/magenta spots per cell in (C). Unpaired Welch's t-test; mean (min-max),  $**P < 0.01$ . (E) ASGP-R western blot of PM samples isolated from WT and Rab3D-KO mice and treated with Endo-H glycosidase (top panel) and sialidase (low panel). (F) ASGP-R western blot of PM samples isolated from hepatocytes of control and alcohol-fed rats, treated with sialidase. Asterisks in (E) and (F) indicate cleaved ASGP-R fragments. (G) Rab3D western blot of the lysates from control and EtOH-treated VA-13 cells transfected with pET28a-LIC empty vector and EtOH-treated VA-13 cells transfected with Rab3D plasmid. (H) ASGP-R western blot of PM samples from cells described in (G); E-cadherin is a PM loading control. Abbreviation: N, nucleus.

## Discussion

The study of ASGP-R is significant due to its clinical implications for patients with ALD and the capacity to import large molecules across the PM, making ASGP-R an excellent target for drug delivery. In EtOH-treated hepatocytes, we identified the mechanism of ASGP-R delivery to the cell surface through ER-PM junctions (Fig. 8). Using Rab3D-KO mice, we found unequivocal evidence that Rab3D is critical for Golgi organization, and deficiency in this GTPase stimulates trafficking opportunities for ASGP-R. Although ER-PM contact sites have

been reported in many cells with the roles of  $\text{Ca}^{2+}$  sequestration, signaling pathway facilitation, and lipid transfer directly to the PM,<sup>(45,46)</sup> it is unclear what specific roles ER-PM junctions hold in liver cells. We speculate that the increase in contact sites in EtOH-treated cells is a compensatory mechanism for the hepatocytes to adapt to ER stress.<sup>(47)</sup> In addition to UPR and ER-associated degradation, ER-PM junctions may help unload proteins arrested in the ER. Given that abnormally glycosylated ASGP-R lose ligand-binding capacity,<sup>(44)</sup> secretion appears to be a choice for the receptors that reached the cell surface. Indeed, the observations in different organs regarding

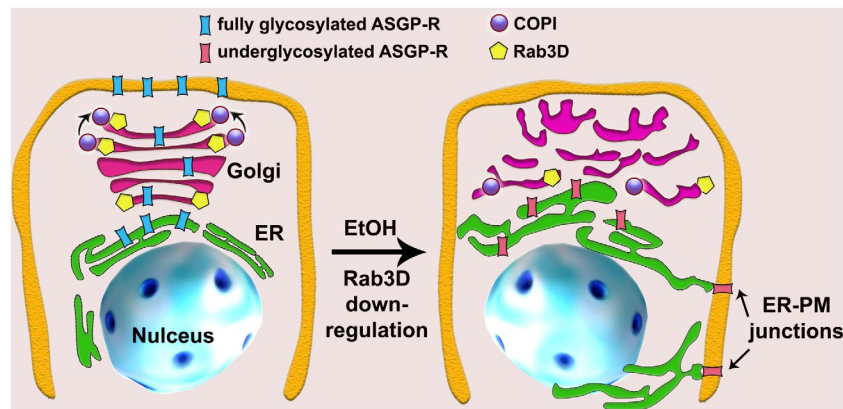


**FIG. 8.** The proposed model of EtOH-induced ASGP-R rerouting. Under normal circumstances, ASGP-R is delivered to the cell surface through canonical anterograde transportation. Rab3D is distributed primarily on *cis*-faces and *trans*-faces of Golgi. EtOH treatment induces Golgi disorganization. Rab3D down-regulation results in its deficiency in *trans*-Golgi, which, in turn, impairs intra-Golgi trafficking of COPI vesicles. ER-PM junctions serve as an alternative trafficking mechanism for abnormally glycosylated ASGP-R.

the secretion of proteins bypassing Golgi suggest that this would be the case<sup>(48)</sup>; however, this possibility for hepatic proteins remains to be investigated.

In sum, our findings suggest that one of the major deleterious effects of alcohol on intracellular trafficking in hepatocytes is mediated through Rab3D down-regulation and *trans*-Golgi disorganization. Future work will also be focused on elucidating the nature of alcohol-induced ER-PM connections for the development of a target therapy of ALD.

## REFERENCES

- Shepard BD, Fernandez DJ, Tuma PL. Alcohol consumption impairs hepatic protein trafficking: mechanisms and consequences. *Genes Nutr* 2010;5:129-140.
- Petrosyan A, Cheng PW, Clemens DL, Casey CA. Downregulation of the small GTPase SAR1A: a key event underlying alcohol-induced Golgi fragmentation in hepatocytes. *Sci Rep* 2015;5:17127.
- Ozeki S, Cheng J, Tauchi-Sato K, Hatano N, Taniguchi H, Fujimoto T. Rab18 localizes to lipid droplets and induces their close apposition to the endoplasmic reticulum-derived membrane. *J Cell Sci* 2005;118:2601-2611.
- Rasineni K, McVicker BL, Tuma DJ, McNiven MA, Casey CA. Rab GTPases associate with isolated lipid droplets (LDs) and show altered content after ethanol administration: potential role in alcohol-impaired LD metabolism. *Alcohol Clin Exp Res* 2014;38:327-335.
- Schroeder B, Schulze RJ, Weller SG, Sletten AC, Casey CA, McNiven MA. The small GTPase Rab7 as a central regulator of hepatocellular lipophagy. *Hepatology* 2015;61:1896-1907.
- Li Q, Wang J, Wan Y, Chen D. Depletion of Rab32 decreases intracellular lipid accumulation and induces lipolysis through enhancing ATGL expression in hepatocytes. *Biochem Biophys Res Commun* 2016;471:492-496.
- Zeigerer A, Gilleron J, Bogorad RL, Marsico G, Nonaka H, Seifert S, et al. Rab5 is necessary for the biogenesis of the endolysosomal system in vivo. *Nature* 2012;485:465-470.
- Drizyte-Miller K, Chen J, Cao H, Schott MB, McNiven MA. The small GTPase Rab32 resides on lysosomes to regulate mTORC1 signaling. *J Cell Sci* 2020;133:jcs236661.
- Liu S, Storrie B. Are Rab proteins the link between Golgi organization and membrane trafficking? *Cell Mol Life Sci* 2012;69:4093-4106.
- Petrosyan A, Holzapfel MS, Muirhead DE, Cheng PW. Restoration of compact Golgi morphology in advanced prostate cancer enhances susceptibility to galectin-1-induced apoptosis by modifying mucin O-glycan synthesis. *Mol Cancer Res* 2014;12:1704-1716.
- Bard F, Casano L, Mallabiabarrena A, Wallace E, Saito K, Kitayama H, et al. Functional genomics reveals genes involved in protein secretion and Golgi organization. *Nature* 2006;439:604-607.
- Dejgaard SY, Murshid A, Erman A, Kızılay Ö, Verbich D, Lodge R, et al. Rab18 and Rab43 have key roles in ER-Golgi trafficking. *J Cell Sci* 2008;121:2768-2781.
- Petrosyan A, Casey CA, Cheng PW. The role of Rab6a and phosphorylation of non-muscle myosin IIA tailpiece in alcohol-induced Golgi disorganization. *Sci Rep* 2016;6:31962.
- Casey CA, Thomes P, Manca S, Petrosyan A. Giantin is required for post-alcohol recovery of Golgi in liver cells. *Biomolecules* 2018;8:150.
- Frisbie CP, Lushnikov AY, Krasnoslobodtsev AV, Riethoven JM, Clarke JL, Stepchenkova EI, et al. Post-ER stress biogenesis of Golgi is governed by giantin. *Cells* 2019;8:1631.
- Larkin JM, Woo B, Balan V, Marks DL, Oswald BJ, LaRusso NF, et al. Rab3D, a small GTP-binding protein implicated in regulated secretion, is associated with the transcytotic pathway in rat hepatocytes. *Hepatology* 2000;32:348-356.
- Valentijn JA, van Weeren L, Ultee A, Koster AJ. Novel localization of Rab3D in rat intestinal goblet cells and Brunner's gland acinar cells suggests a role in early Golgi trafficking. *Am J Physiol Gastrointest Liver Physiol* 2007;293:G165-G177.
- Jena BP, Gumkowski FD, Konieczko EM, von Mollard GF, Jahn R, Jamieson JD. Redistribution of a rab3-like GTP-binding

- protein from secretory granules to the Golgi complex in pancreatic acinar cells during regulated exocytosis. *J Cell Biol* 1994;124:43-53.
- 19) Pavlos NJ, Xu J, Riedel D, Yeoh JSG, Teitelbaum SL, Papadimitriou JM, et al. Rab3D regulates a novel vesicular trafficking pathway that is required for osteoclastic bone resorption. *Mol Cell Biol* 2005;25:5253-5269.
  - 20) Evans E, Zhang W, Jerdeva G, Chen CY, Chen X, Hamm-Alvarez SF, et al. Direct interaction between Rab3D and the polymeric immunoglobulin receptor and trafficking through regulated secretory vesicles in lacrimal gland acinar cells. *Am J Physiol Cell Physiol* 2008;294:C662-C674.
  - 21) Riedel D, Antonin W, Fernandez-Chacon R, Alvarez de Toledo G, Jo T, Geppert M, et al. Rab3D is not required for exocrine exocytosis but for maintenance of normally sized secretory granules. *Mol Cell Biol* 2002;22:6487-6497.
  - 22) Martelli AM, Baldini G, Tabellini G, Koticha D, Bareggi R, Baldini G. Rab3A and Rab3D control the total granule number and the fraction of granules docked at the plasma membrane in PC12 cells. *Traffic* 2000;1:976-986.
  - 23) Kogel T, Rudolf R, Hodneland E, Copier J, Regazzi R, Tooze SA, et al. Rab3D is critical for secretory granule maturation in PC12 cells. *PLoS One* 2013;8:e57321.
  - 24) van Weeren L, de Graaff AM, Jamieson JD, Batenburg JJ, Valentijn JA. Rab3D and actin reveal distinct lamellar body subpopulations in alveolar epithelial type II cells. *Am J Respir Cell Mol Biol* 2004;30:288-295.
  - 25) Pavlos NJ, Cheng TS, Qin A, Ng PY, Feng H-T, Ang ESM, et al. Tctex-1, a novel interaction partner of Rab3D, is required for osteoclastic bone resorption. *Mol Cell Biol* 2011;31:1551-1564.
  - 26) Ashwell G, Harford J. Carbohydrate-specific receptors of the liver. *Annu Rev Biochem* 1982;51:531-554.
  - 27) Tworek BL, Tuma DJ, Casey CA. Decreased binding of asialoglycoproteins to hepatocytes from ethanol-fed rats. Consequence of both impaired synthesis and inactivation of the asialoglycoprotein receptor. *J Biol Chem* 1996;271:2531-2538.
  - 28) Casey CA, Kragoskowsky SL, Sorrell MF, Tuma DJ. Chronic ethanol administration impairs the binding and endocytosis of asialo-orosomucoid in isolated hepatocytes. *J Biological Chemistry* 1987;262:2704-2710.
  - 29) Manca S, Frisbie CP, LaGrange CA, Casey CA, Riethoven JM, Petrosyan A. The role of alcohol-induced golgi fragmentation for androgen receptor signaling in prostate cancer. *Mol Cancer Res* 2019;17:225-237.
  - 30) Kubyskhin AV, Fomochkina II, Petrosyan AM. The impact of alcohol on pro-metastatic N-glycosylation in prostate cancer. *Krim Z Eksp Klin Med* 2018;8:11-20.
  - 31) Burgess JB, Baenziger JU, Brown WR. Abnormal surface distribution of the human asialoglycoprotein receptor in cirrhosis. *Hepatology* 1992;15:702-706.
  - 32) Hilgard P, Schreiter T, Stockert RJ, Gerken G, Treichel U. Asialoglycoprotein receptor facilitates hemolysis in patients with alcoholic liver cirrhosis. *Hepatology* 2004;39:1398-1407.
  - 33) McVicker BL, Tuma DJ, Kubik JA, Hindemith AM, Baldwin CR, Casey CA. The effect of ethanol on asialoglycoprotein receptor-mediated phagocytosis of apoptotic cells by rat hepatocytes. *Hepatology* 2002;36:1478-1487.
  - 34) McVicker BL, Tuma DJ, Kharbanda KK, Kubik JL, Casey CA. Effect of chronic ethanol administration on the in vitro production of proinflammatory cytokines by rat Kupffer cells in the presence of apoptotic cells. *Alcohol Clin Exp Res* 2007;31:122-129.
  - 35) Mohr AM, Gould JJ, Kubik JL, Talmon GA, Casey CA, Thomas P, et al. Enhanced colorectal cancer metastases in the alcohol-injured liver. *Clin Exp Metastasis* 2017;34:171-184.
  - 36) Clemens DL, Forman A, Jerrells TR, Sorrell MF, Tuma DJ. Relationship between acetaldehyde levels and cell survival in ethanol-metabolizing hepatoma cells. *Hepatology* 2002;35:1196-1204.
  - 37) McVicker BL, Tuma DJ, Kubik JL, Tuma PL, Casey CA. Ethanol-induced apoptosis in polarized hepatic cells possibly through regulation of the Fas pathway. *Alcohol Clin Exp Res* 2006;30:1906-1915.
  - 38) Rasineni K, Penrice DD, Natarajan SK, McNiven MA, McVicker BL, Kharbanda KK, et al. Alcoholic vs non-alcoholic fatty liver in rats: distinct differences in endocytosis and vesicle trafficking despite similar pathology. *BMC Gastroenterol* 2016;16:27.
  - 39) Casey CA, Bhat G, Holzapfel MS, Petrosyan A. Study of ethanol-induced Golgi disorganization reveals the potential mechanism of alcohol-impaired N-glycosylation. *Alcohol Clin Exp Res* 2016;40:2573-2590.
  - 40) Ji C. Mechanisms of alcohol-induced endoplasmic reticulum stress and organ injuries. *Biochem Res Int* 2012;2012:216450.
  - 41) Fang J, Liu M, Zhang X, Sakamoto T, Taatjes DJ, Jena BP, et al. COPII-dependent ER export: a critical component of insulin biogenesis and beta-cell ER homeostasis. *Mol Endocrinol* 2015;29:1156-1169.
  - 42) Amodio G, Venditti R, De Matteis MA, Moltedo O, Pignataro P, Remondelli P. Endoplasmic reticulum stress reduces COPII vesicle formation and modifies Sec23a cycling at ERESs. *FEBS Lett* 2013;587:3261-3266.
  - 43) Petrosyan A. Unlocking Golgi: Why does morphology matter? *Biochemistry (Mosc)* 2019;84:1490-1501.
  - 44) Paulson JC, Hill RL, Tanabe T, Ashwell G. Reactivation of asialo-rabbit liver binding protein by resialylation with beta-D-galactoside alpha2 leads to 6 sialyltransferase. *J Biol Chem* 1977;252:8624-8628.
  - 45) Suski JM, Lebedzinska M, Wojtala A, Duszynski J, Giorgi C, Pinton P, et al. Isolation of plasma membrane-associated membranes from rat liver. *Nat Protoc* 2014;9:312-322.
  - 46) Saheki Y, De Camilli P. Endoplasmic reticulum-plasma membrane contact sites. *Annu Rev Biochem* 2017;86:659-684.
  - 47) Manford AG, Stefan CJ, Yuan HL, Macgurn JA, Emr SD. ER-to-plasma membrane tethering proteins regulate cell signaling and ER morphology. *Dev Cell* 2012;23:1129-1140.
  - 48) Grieve AG, Rabouille C. Golgi bypass: skirting around the heart of classical secretion. *Cold Spring Harb Perspect Biol* 2011;3:a005298.

## Supporting Information

Additional Supporting Information may be found at [onlinelibrary.wiley.com/doi/10.1002/hep4.1811/supinfo](http://onlinelibrary.wiley.com/doi/10.1002/hep4.1811/supinfo).